Simulation and dynamics of entropy-driven, molecular self-assembly processes

Bernd Mayer,[1,*,†] Gottfried Köhler,[1] and Steen Rasmussen[2,3,*,‡]

[1]*Institut für Theoretische Chemie und Strahlenchemie, Universität Wien, UZAII, Althanstrasse 14, A-1090 Wien, Austria*
[2]*Santa Fe Institute, 1399 Hyde Park Road, Santa Fe, New Mexico 87501*
[3]*TSA-DO/SA MS-M997 and CNLS MS-B258, Los Alamos National Laboratory, Los Alamos, New Mexico 87545*

Molecular self-assembly is frequently found to generate higher-order functional structures in biochemical systems. One such example is the self-assembly of lipids in aqueous solution forming membranes, micelles, and vesicles; another is the dynamic formation and rearrangement of the cytoskeleton. These processes are often driven by local, short-range forces and therefore the dynamics is solely based on local interactions. In this paper, we introduce a cellular automata based simulation, the lattice molecular automaton, in which data structures, representing different molecular entities such as water and hydrophilic and hydrophobic monomers, share locally propagated force information on a hexagonal, two-dimensional lattice. The purpose of this level of description is the simulation of entropic and enthalpic flows in a microcanonical, molecular ensemble to gain insight about entropy-driven processes in molecular many-particle systems. Three applications are shown, i.e., modeling structural features of a polar solvent, cluster formation of hydrophobic monomers in a polar environment, and the self-assembly of polymers. Processes leading to phase separation on a molecular level are discussed. A thorough discussion of the computational details, advantages, and limitations of the lattice molecular automaton approach is given elsewhere [B. Mayer and S. Rasmussen (unpublished)]. [S1063-651X(97)06703-2]

I. INTRODUCTION

A. Biological motivation

Many processes in biomolecular systems lack global, interfering control. The system dynamics is solely based on local interactions, providing, based on immediate reactions on environmental changes, the necessary flexibility and mean stability of the whole system. Considering the prokaryotic cell as a hierarchically structured, dynamical system, it is possible to characterize specific, functionally linked, mesoscopic complexes. One of these compounds is the semipermeable membrane separating space into an inside and an outside [2]. These membranes consist of a certain type of amphiphilic polymers (hydrophilic head, hydrophobic tail) acting in the highly polar environment of water.

A basic component as a membrane is, from the theoretical viewpoint, characterizable as a higher order, emergent structure [3,4], dynamically formed by interactions between lipids due to an entropy gradient arising from the structured polar (water) environment. Phase separation of, e.g., lipids in water and a concomitant ordering to vesicles and micelles is a spontaneous process lasting from seconds to minutes [5–8].

The resulting higher-order structures have themselves rich dynamics, e.g., turnover (flip-flop mechanism) of single lipids within membranelike structures. This flexibility is of major importance to maintain functionality in a cell membrane, which hosts systems at higher hierarchical levels such as the complex for photosynthesis [9].

The hydrophobic effect (HE), describing mainly an entropic effect, seems to be of fundamental importance in the self-organization of such biological systems [10]. Various circumstances lead to the formulation of a hydrophobic *effect* rather than a hydrophobic *force*: The most reliable indication that it is indeed a hydrophobic effect comes from thermodynamics, considering free energy, enthalpy, and entropy of solvation processes

$$\Delta G = \Delta H - T\Delta S, \tag{1}$$

where ΔG is the change of free energy, ΔH is the change of enthalpy, T is the temperature, and ΔS is the change of entropy.

It is experimentally known that the free-energy change of dissolution of hydrophobic molecules in a polar solvent is positive, although the change in enthalpy (at room temperature) is often zero or even negative [11]. Considering that liquid water has to some extent quasicrystalline features with highly ordered regions [12,13], the HE is believed to be based on a change of the water structure in the vicinity of hydrophobic surfaces and a concomitant decrease of entropy. Following this model, the solvent is forced to form a ''cave around'' the hydrophobic surface. This reaction, often referred to as hydrophobic solvation, is accomplished by a different dynamics of the solvent in the vicinity of hydrophobic surfaces compared to the bulk solvent phase: The accessibility of microstates decreases and thus the entropy decreases. Due to the high surface tension of such a molecular cave, the solvent tends to ''minimize'' its contact surface to hydrophobic molecules, which leads eventually to the phase separation between water and hydrophobic molecules.

Entropy gradients and resulting phase separation are therefore based on effects *generated* by the system dynamics. They are not observable as explicit interaction forces, but are the result of basic molecular interactions between hydro-

————
*Authors to whom correspondence should be addressed.
†Electronic address: bernd@asterix.msp.univie.ac.at
‡Electronic address: steen@lanl.gov

phobic particles and the polar solvent. They are *emergent* properties.

B. Simulation of molecular systems

1. Molecular dynamics and Monte Carlo methods

Recently, various methods have been applied to simulate structural and dynamic properties of macromolecular systems. One such example is genetic algorithms [14], implementing formal criteria of Darwinian evolution through a fitness function (which is in analogy to an energy function). With such a method it is, for instance, possible to determine secondary structure motifs of polymers as proteins. However, the classical tools to simulate large molecular systems are deterministic routines such as molecular dynamics, solving Newton's equations of motion [15], or stochastic algorithms such as the dynamic Monte Carlo method [16]. These tools are based on force field calculations considering the terms

$$V_{\text{total}} = \sum_{\text{bonds}} V^{i,j} + \sum_{\text{bond angle}} V^{i,j,k} + \sum_{\text{torsion}} V^{i,j,k,l}$$
$$+ \sum_{\text{electrostatic}} V^{i,j} + \sum_{\text{van der Waals}} V^{i,j}, \qquad (2)$$

where V is the potential energy and i,j,k,l are atoms or atom groups. The total potential energy V_{total} of a system with n atoms is calculated as a sum of individual contributions arising from pairwise intra- and intermolecular interactions. Other types of force fields using different intra- and intermolecular potentials, such as knowledge-based potentials or mean-field minimization methods, are discussed in Ref. [17]. Recent investigations have proven the importance of weak intermolecular interactions of the van der Waals type including a polar solvent for general molecular recognition processes [18,19]. A total potential energy of a molecular system in solution V_{total} has to be calculated as a sum of conformational and solvation energies

$$V_{\text{total}} = V_{\text{conformational}} + V_{\text{solvation}}. \qquad (3)$$

Potential energies arising from solvation are calculated as pairwise interactions based on electrostatic and van der Waals terms represented as Coulomb and Lennard-Jones potentials [20] or as changes in the free energy in a continuum approximation [19]. The pair potentials used in a representation of a solvent do not reproduce cooperative effects as they occur in the hydrogen bonded network of water.

There are three major problems associated with the formulation of molecular dynamics as noted above. (i) Using an atomic level of description instead of a molecular (at the monomer) level of description makes a simulation of molecular self-assembly more complicated than it need be. With such a low-level description it is not possible to simulate, for instance, processes ranging in a time scale up to minutes like the self-assembly of lipid membranes. The second problem with these descriptions on the atomic level is the high complexity of the simulator itself, for instance, shown in the protein folding problem [21]. (ii) Using a (pure) mechanistic instead of cellular automata modeling technique

makes the updating of the system too cumbersome and slower than necessary, since one, in principle, needs to make $\sim n^2$ calculations (every pairwise interaction) in a system with n particles instead of $\sim n$ calculations. (iii) Using real (continuous) variables instead of integers or bit operations also slows down the computation when using digital computers. For a further discussion of these issues we refer to [22].

An excellent overview describing lattice models to simulate macromolecular systems is given in Ref. [23]. Such Ising spin based models are capable of generating generic phenomena of, e.g., phase separation.

2. Lattice molecular automaton

The lattice molecular automaton (LMA) is an extention of the lattice polymer automata (LPA) [22] and they are both made in the spirit of the lattice gas automata (LGA) [24]. Both the LGA and the LPA have proven to be capable of generating macroscopic effects based on a microscopic, discrete system representation. In the LMA approach, molecules also interact on a hexagonal lattice with toroidal boundary conditions. This lattice type has proven to be suitable to avoid anisotropic effects [24]. The molecular entities and vacuum are encoded in data structures on each lattice site to ensure optimal parallel processing. Kinetic- and potential-energy terms are implemented in the LMA via information particles describing an artificial physics within a microcanonical ensemble: constant volume, constant number of molecules, and constant energy. The inner structure of molecules is not considered; only intermolecular interactions model the dynamics of the system. The forces in the system are determined by a propagation of information or ''force,'' particles between neighboring data structures. Due to the explicit discrete character of these information particles, discrete state functions of the data structures can be evaluated (counted) to calculate thermodynamic properties such as entropy and enthalpy.

II. THE LATTICE MOLECULAR AUTOMATON CONCEPT

A. Artificial physics in the LMA

The dynamics of a molecular system depends on kinetic-energy terms and on the relative molecular position on a potential-energy hypersurface. In a nondissipative system, the basic conservation laws have to be fulfilled. That means keeping mass M, momentum P, and the total energy E_{total} constant. What is ''optimized'' in the equilibrium of such a system is the relative position of molecules, leading, depending on the thermal state, to a certain minimum of the sum potential energy

$$V_{\text{total}} = \sum_{i=1}^{n} \sum_{j=1}^{k} V^{j,i}, \qquad (4)$$

where $V^{j,i}$ is the local potential-energy situation, n is the number of molecules, and k is the number of potential-energy terms. In the LMA, as we shall see, a Boltzmann distribution of kinetic energies drives the many-particle system into locally stable, sum energy configurations.

1. Implementation of kinetic energy

Each molecule on the hexagonal lattice has six directions of translation. Each direction is, per definition, independent and occupied by a Boltzmann distribution of kinetic energies. For all particles, directions, and times, the kinetic energy for each direction of a translation is larger than zero. In the case of a collision process, the kinetic energies are distributed between the respective molecules following a collision model for hard spheres. [This formulation describes pairwise collision processes correctly (conservation of momentum and energy), but only approximates more complicated collision situations including more than two molecules or molecules in polymers. See also Sec. IV D 3 for more details.]

The only way to distribute kinetic energies is via collision processes. During a free translation of a molecule, all currently occupied kinetic-energy levels are conserved and the molecule is characterized as an isolated particle. The overall (global) thermal state of the system, as the sum kinetic energy, stays constant in time. This implies also an overall conservation of momentum in time for each of the six independently treated, principle directions on the hexagonal lattice. The kinetic-energy distribution is identical for all considered molecular types, further assuming equal mass for water and hydrophobic and hydrophilic monomers.

2. Implementation of potential energy

The implementation of a potential-energy term is necessary to characterize special physicochemical features of the different molecular types. Let us consider a model system for a lipid-water mixture consisting of the following molecules [see also the schematic drawings in Figs. 1(b)1 and 1(c)1]: solvent, water H_2O and polymer, fatty acid CH_3-CH_2-CH_2-CH_2-COOH. The most important term for calculating potential energies between uncharged model polymers are electrostatic and van der Waals terms [see also Eq. (2)] [25]. In the present LMA, three forces of this type are included to characterize hydrophilic and hydrophobic properties of monomers in the polymer and water: (i) dipole-dipole interactions as well as hydrogen bonds for water-water and water–hydrophilic-monomer interactions, (ii) dipole–induced-dipole interactions for water-hydrophobic monomer and hydrophilic–hydrophobic-monomer interactions, and (iii) induced-dipole–induced-dipole interactions for hydrophobic-monomer–hydrophobic-monomer interactions. One important aspect for the following considerations is the comparable distance dependence of all three forces: They are short ranged in aqueous solution. The relative strength of the three different interactions is, however, different, as the potential-energy gain from a typical H bond is around −2 kcal/mol; the other interactions contribute with energies in the range of −0.5 kcal/mol.

The important features of a water model are the highly polar character of water and the ability to form stable hydrogen bonds (H bonds), i.e., to have three defined interaction directions (two hydrogens and one oxygen). The high degree of order within liquid water is mainly based on these comparably strong H bonds [12]. Hydrophilic monomers are either charged or have the capability to form H bonds, such as the carboxyl group in our model polymer. The interactions between hydrophobic and hydrophilic molecules are weaker

and mainly based on the polarizability of the hydrophobic molecules. Interactions between hydrophobic moieties are comparably strong since electrostatic forces are not shielded by a water shell. The dielectric constant ϵ_τ decreases from 80 in bulk water phase to less than 10 between two neighboring hydrophobic surfaces. The total potential energy V_{total} of our model system with n molecules is thus described by

$$V_{total} = \sum_{i=1}^{n} \sum_{j=1}^{6} V_{dip\text{-}dip,H\,bond}^{j,i} + \sum_{i=1}^{n} \sum_{j=1}^{6} V_{dip\text{–}ind\text{-}dip}^{j,i}$$

$$+ \sum_{i=1}^{n} \sum_{j=1}^{6} V_{ind\text{-}dip\text{–}ind\text{-}dip}^{j,i}, \qquad (5)$$

where the sum is over all molecules and over the neighborhood (six directions) for each molecule.

In the LMA simulation environment, dipole-dipole interactions and H bonds account for a (dimensionless) value of −5 and all other binding interactions for a value of −1 for the total potential energy. Water molecules can, summing over the six principle directions, be stabilized by a value of −18 (three H bonds and three dipole–induced-dipole interactions), hydrophilic monomers by a value of −14 (two hydrogen bonds and four dipole–induced-dipole interactions), and hydrophobic monomers by a value of −6 (six induced-dipole–induced-dipole and/or dipole–induced-dipole interactions). The relative strength of these interactions is chosen according to corresponding experimentally determined values as noted above.

In the LMA approach, these potential energies provide attractive binding or repelling forces. They influence the occupation time of a given molecule on a particular lattice location with a given kinetic-energy distribution. The higher the potential-energy value, the more likely it is for a molecule to stay at that given location. If the kinetic energy of a molecule exceeds the sum potential energy at a given location, the molecule will not stay, but continue in the direction where it has its highest kinetic energy. If, for instance, a hydrogen bond is formed, the binding energy of this particular bond is stored as internal energy in the bonded molecules. In the case of a collision, the propagated kinetic energy is compared to the internal (binding) energy. If gains from kinetic energy are larger than contributions from binding, the particular bonds break up.

III. INFORMATION DYNAMICS: THE LMA UPDATE CYCLE

The discrete field automata are based on the assumption that all molecular interactions can be modeled by mediating particles [22]. Both matter and fields are interpreted as "information particles" that propagate locally along the edges of a lattice and interact with one another at nodes, as in a LGA [26]. Thus the rules that generate the dynamics are (i) the rules that propagate the information particles that depend on the current state of the current site and (ii) the rules that evaluate the newly propagated information together with local states, and (iii) the chosen update schedule. Unlike a standard LGA and as in the LPA [22] several different types of information particles are used, so the structure of a node is more complicated than the simple six-bit register required
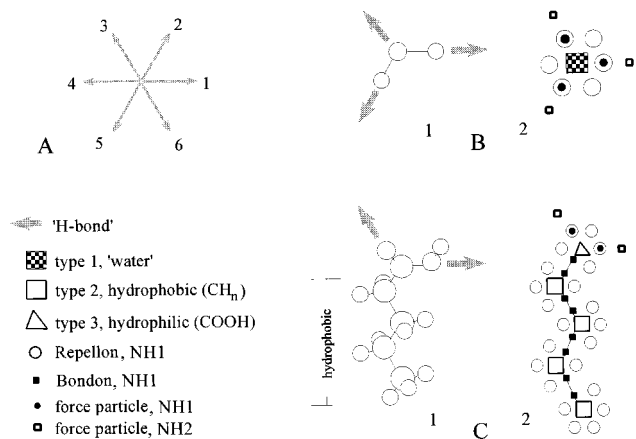
FIG. 1. (a) Six principle directions on a hexagonal lattice. (b)1 and (c)1 Schematic representation of water and a polymer in the LMA. (b)2 and (c)2 Propagation of information particles to maintain the excluded volume (repellons), bonds between monomers in polymers (bondons), and force particles (attractons) generating type specific force fields, to neighborhoods (NH) 1 and 2 on the hexagonal lattice, respectively.

FIG. 2. Particle propagation for two water molecules in position (i,j), $(i,j+1)$ on the hexagonal lattice: (a) propagation of repellons to NH1, ensuring the excluded volume; (b) and (c) propagation of force particles (attractons) to NH1 and NH2 describing a type specific force field.

for a minimal LGA. The molecular model to be discussed here is formulated on a two-dimensional hexagonal lattice [see Fig. 1(a)].

Figures 1(b)2 and 1(c)2 depict the abstract LMA representation of water and monomers in a polymer. All stored information in the data structures is propagated to a given neighborhood (NH) on the hexagonal lattice. Excluded-volume particles, ''repellons,'' are propagated to neighborhood 1. To prevent polymers from breaking up, ''bondons'' are propagated to neighboring monomers in the polymer. The bond length between two monomers in a polymer is fixed to the length of one lattice site. The force particles, propagated to neighborhoods 1 and 2, represent the van der Waals properties of the molecular compounds. They also mimic the H-bonding capabilities of water and hydrophilic monomers, as indicated by the arrows.

The transmission of the force particles between the molecules enables an update of each molecule using only local information. After the information particle transport steps, each lattice site can be updated independently. The force-communicating particles propagate locally, that is, between neighboring lattice sites. A variety of molecular interactions may be formulated by choosing the mediating particles properly. For instance, a polymer must obey a connectivity constraint between its monomers and all molecules must obey an excluded-volume constraint. The chemical information hydrophobicity and hydrophilicity as well as the structural information on water are characterized by these force particles. As an example, the propagation of force particles of two water molecules in positions (i,j) and $(i,j+1)$ on the lattice is shown in Fig. 2.

In Fig. 2(a) two data structures representing water are depicted after the propagation of the excluded-volume information particles, the repellons. These particles mimic a hard-sphere collision between two molecular surfaces in close contact. Their propagation is also the basis for the exchange of kinetic energies in a collision process. In Fig. 2(b) the propagation step of force particles, the attractions, is shown.
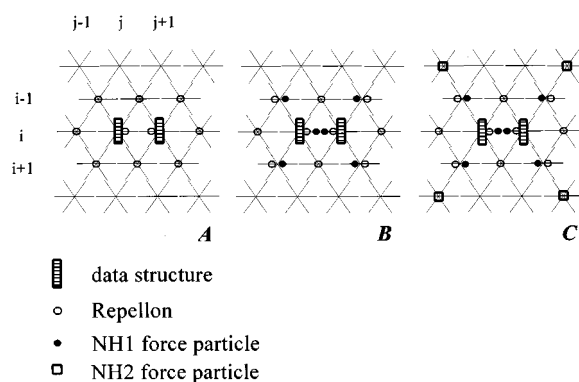
In a first step, these force particles are propagated to neighborhood 1 and in a second step to neighborhood 2 [see Fig. 2(c)]. These attractions represent the binding sites for hydrogen bonds as also denoted schematically in Figs. 1(b)1, 1(b)2, 1(c)1, and 1(c)2. As can be seen in Fig. 2(c), the NH2 propagation step of the force particles does not take place in direction 1 for the molecule on the location (i,j) and also not in direction 4 for the molecule on $(i,j+1)$. This mimics the high dielectric constant in bulk water. Force particles (representing an electric field) are shielded by water, but not by hydrophobic monomers (see also Sec. II A 2).

In summary, a simulation update consists of the following steps: (i) propagation of molecular types and redistribution of kinetic energies, (ii) construction of type specific force fields, (iii) calculation of potential energies, (iv) calculation of the most proper move direction, (v) readjustment of bonds in polymers according to the move direction, and (vi) movement of the molecule and clearing the lattice for the new update. A detailed description of a full LMA update is presented in Ref. [1].

IV. LMA DYNAMICS: MOLECULAR DYNAMICS AND MOLECULAR SELF-ASSEMBLY

A. Representation of the polar solvent

A radial distribution function (RDF) g_r is a quantity that checks basic ''geometrical'' features of the solvent in a system. This function gives a probability P of finding a molecule in a certain neighborhood distance r. For liquid water, experimentally determined RDFs (by x-ray scattering) show a peak at 0.25 nm (H-bond distance) and smaller peaks for the next theoretical H-bond distances (temperature dependent). This function reflects the ordered structure of the neighborhood of a particular water molecule in the liquid phase, mainly based on the formation of hydrogen bonds.

Figure 3 shows a RDF obtained by a LMA simulation of a polar solvent such as water [see Figs. 1(b)1 and 1(c)1] after 10^5 simulation steps, where 50% of the lattice sites are occupied with water. The probability g_r in the range [0,1] is plotted versus the neighborhood distance on the hexagonal lattice. There is an increased probability of finding another
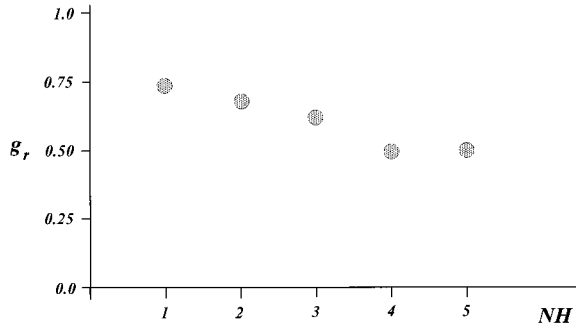
FIG. 3. Radial distribution function g_r of a LMA water simulation (for definition see the text): 50% of the data structures on the lattice are covered with water, 50% are empty. The figure is based on a set of 10^4 molecules after 10^5 simulation steps.

FIG. 4. Two snapshots of the LMA water representation in equilibrium (a) at time $t=10^5$ simulation steps and (b) at time $t=10^5+10$ steps. Data structures representing water are denoted as circles.

water molecule for neighborhoods 1, 2, and 3 [e.g., the lattice positions $(i,j+1)$, $(i,j+2)$, and $(i,j+3)$ in direction 1] since $g_r > 0.5$. This RDF shows the comparably higher local clustering of water molecules based on the H-bond binding energies. Without implementation of these stabilizing energy contributions, the RDF shows no peaks characterizing an ordered neighborhood and the molecules are randomly distributed throughout the lattice ($g_r=0.5$ with a 50% lattice occupation). The turnover rate (change of molecule position per time step) is in the range of 30%, but the general shape of the RDF remains unchanged in time.

Figure 4 shows two snapshots [time difference of ten simulation steps between (a) and (b)] of a water simulation generating the RDF given in Fig. 3, where 50% of the lattice sites are occupied with water (denoted by open circles). The formation of local, irregular clusters is shown, but within the next ten time steps a global rearrangement of cluster structures takes place. The crucial point to obtain this behavior in the simulation system is an appropriate balance of kinetic and binding (potential) energies.

B. Balance between kinetic and potential energies

The summed binding energy $V_{b,\text{total}}$ and the summed kinetic energy K_{total} are given by

$$V_{b,\text{total}} = \sum_{k=1}^{n} \sum_{l=1}^{6} |V_{\text{binding}}^{l,k}|, \qquad (6)$$

$$K_{\text{total}} = \sum_{k=1}^{n} \sum_{l=1}^{6} K^{l,k}, \qquad (7)$$

where l is the index over the six principle lattice directions and k is the index over n molecules. In a nondissipative system, the total inner energy is constant. In the LMA, K_{total} is by definition constant. The summed binding energy is in the mean constant in the equilibrium situation. The value of $V_{b,\text{total}}$ will in general decrease over time until a (local) minimum value has been obtained that corresponds to equilibrium. The yield of potential energy is implicitly stored in the system (see also Sec. V).

The mean value of $V_{b,\text{total}}$ is proportional to the fixed value of the thermal state K_{total} of the whole system
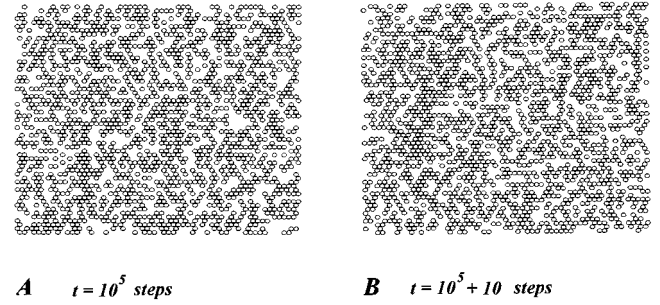
$$K_{\text{total}} = a_{\text{global}} V_{b,\text{total}}, \qquad (8)$$

where a_{global} is the global proportionality factor. The global proportionality factor a_{global} is proportional to the temperature of the system (high kinetic energy corresponds to high temperature) and defines intrinsically the dynamics of the system: $a_{\text{global}} < 1$ fixes the system in a local minimum where the variation of particle position in time tends towards zero (in analogy to a spin glass at low temperature). To obtain the formation of unstable, but locally ordered clusters, as shown in Fig. 4, a_{global} has to be in a range 3–4 (3.7 for the system shown in Fig. 4). The mean binding energy per lattice site for this water simulation is around 5, summed over the six principle directions. This indicates that an average one H bond is formed per water molecule. The respective value for the mean kinetic energy, again summed over the six directions, is 21. High values of $a_{\text{global}} > 6$ enhance the disorder in the system: The structured radial distribution function, as shown in Fig. 3, vanishes and a random distribution with values near 0.5 is obtained for all neighborhoods. This finding is equivalent to the experimentally determined change of RDF of liquid water at high temperature.

While a_{global} on average is constant in time in equilibrium, the local proportionality $a_{\text{local}}^{(i,j)}$ between $V_b^{(i,j)}$ and $K^{(i,j)}$ at the site (i,j) exhibits strong fluctuations. The values $a_{\text{local}}^{(i,j)}$ of the time series in Fig. 5 (thin line) show the local change of kinetic and binding energies in time (given in simulation steps). They are summed over the six principle directions on the lattice and recorded during 500 time steps in the equilibrated system for one of the water molecules in Fig. 4. These local characteristics of the molecular dynamics differ completely from the global behavior: Fluctuations between binding and kinetic energies characterize the local situation, whereas the relation between these two terms is on average constant in time for the global system (thick line, Fig. 5), showing the global proportionality factor of 3.7, as discussed above. This picture represents the local flow of binding (ordering) and kinetic (disordering) energies on a particular water molecule in the global equilibrium situation. In the case $a_{\text{local}}^{(i,j)} > a_{\text{global}}$, excess kinetic energy drives the molecule into free translation; if $a_{\text{local}}^{(i,j)} < a_{\text{global}}$, the molecule is in the mean fixed on a cluster position in the hydrogen bonded water network. This relationship of the local instability is the cause for the formation of local, unstable clusters in the model for
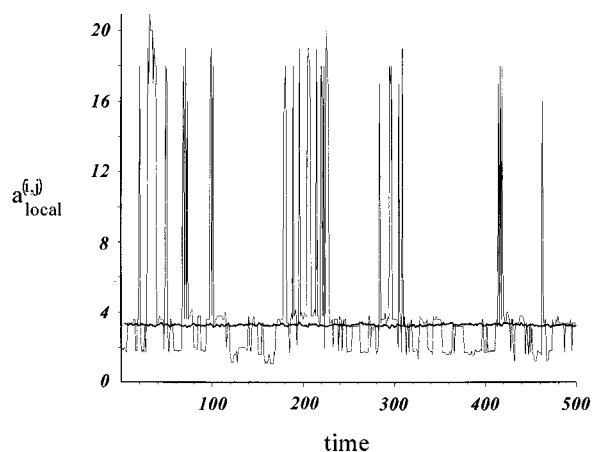
FIG. 5. Evolution of the local proportionality factor $a_{local}^{(i,j)}$ (thin line) and the global proportionality factor a_{global} (thick line) (for definition see the text) for a LMA water simulation during 500 time steps in equilibrium.

a polar solvent like water. In this way the system is tunable between a ''quasicrystal'' phase and a ''gas'' phase by altering a_{global}.

C. Dynamics of hydrophobic monomers in a polar environment

The main type specific feature of hydrophobic monomers in the LMA is the interaction with other hydrophobic monomers according to the induced-dipole–induced-dipole type (see Sec. II A 2). The relative strength of this force in the present LMA setup is set equal to the dipole–induced-dipole interaction between water and hydrophobic monomers. Hydrophobic monomers have therefore no binding preference for water or other hydrophobic monomers.

Figure 6 shows snapshots of a water-hydrophobic monomer system, 10^5 simulation steps after the initial random mixing of both molecular types. 50% of the lattice sites are occupied by molecules. The fraction of hydrophobic monomers (filled circles) is 16% in Fig. 6(a) and 25% in Fig. 6(b). The remaining fractions [34% and 25% in Figs. 6(a) and

A   *t = 10^5 steps*   **B**   *t = 10^5 steps*
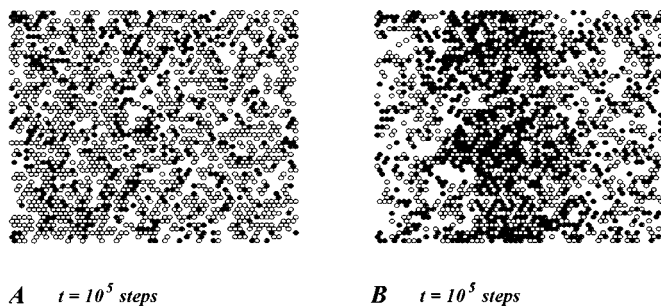
FIG. 6. Snapshots of mixtures of water:hydrophobic monomers after 10^5 updates. (a) 16% hydrophobic monomers, 34% water, 50% empty; (b) 25% hydrophobic monomers, 25% water, 50% empty. Water is denoted as open circles, hydrophobic monomers as filled circles. Cluster formation (phase separation) is occurring for both mixtures, strongest for the mixture with most hydrophobic monomers.

6(b), respectively] is filled with water (open circles). In Fig. 6(a) the mean binding energy [see Eq. (6)] of a hydrophobic monomer, again summed over all six directions, is 2.5 and the value for water is 5.5. The respective values for Fig. 6(b) are 4.2 and 5.7. The mean kinetic energy for both molecular types is again 21 for both simulations. The global proportionality a_{global} is, after 10^5 updates, 4.4 for Fig. 6(a) and 4.2 for Fig. 6(b). The increase of the global proportionality factor (compared to pure water) is mainly due to the loss of hydrogen bonds between water molecules, whose energy contributions are, in this system, only partly counteracted by the binding energy based on water-hydrophobic monomer and hydrophobic-monomer–hydrophobic-monomer interactions. However, the mean stabilization of a water molecule in a mixture is larger than in the bulk (comparing the values of 5.5 and 5.7 for binding energies denoted above with the value 5.0 discussed in Sec. II B).

The hydrophobic monomers (filled circles) start to form clusters in the polar environment and the mean cluster size depends intrinsically on the fraction of water to hydrophobic monomers. The dynamics to form larger clusters is rather slow after the first formation of small clusters as found in Fig. 6(a). This behavior is based on nonlinear kinetics: first the comparably fast formation of small clusters, then the slower diffusion dynamics of these clusters to form larger hydrophobic domains.

The energetic basis of the cluster formation itself is the most interesting part. The clustering takes place, although the binding energy between two hydrophobic monomers is comparably weak, much weaker than the water-water binding (ratio 1:5 in the current setup) and only as strong as the hydrophobic-monomer–water interaction. A hydrophobic molecule has therefore no binding energy preference for water or another hydrophobic monomer, but still clustering occurs. The reason for the starting phase separation is therefore based on the properties of the polar solvent, as will be shown in Sec. V. Complete phase separation can be simulated by increasing the induced-dipole–induced-dipole interaction to a value less than or equal to -2 instead of -1. But already the equal interaction strength between water and hydrophobic monomers as well as between different hydrophobic monomers is sufficient for the clustering.

D. Polymer dynamics in the LMA

1. Hydrophobic and hydrophilic pentamers in a polar environment

The snapshots of Fig. 7 [after (a) 10^3, (b) 5×10^4, and (c) 10^5 updates] of a simulation of five hydrophobic pentamers in the polar solvent show the progress of cluster formation. Filled circles denote hydrophobic monomers, open circles denote water molecules. This clustering of hydrophobic polymers is not an artifact based on the update rules, as can be shown easily when simulating the dynamics of hydrophilic pentamers (which ''like'' to be in contact with water, based on the formation of strong H bonds) in the same setup. Hydrophilic monomers are always completely dissolved by water molecules and take part in the H-bond network. Free hydrophilic monomers and hydrophilic polymers show no cluster formation in the polar solvent. The clusters formed by hydrophobic polymers are not ordered, as there is no addi-
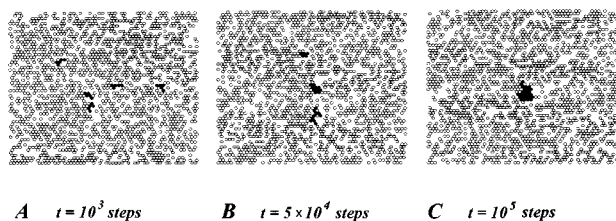
FIG. 7. Cluster formation in a LMA polymer simulation: (a) 10^3 time steps, (b) 5×10^4 time steps, and (c) 10^5 time steps. Hydrophobic monomers in the pentamers are denoted as filled circles, water molecules as open circles.

FIG. 8. Snapshots of typical polymer clusters in a simulation of lipidlike pentamers in a polar environment. The details (a) and (b) (dimers) and (c) (quatermer) are taken from a run simulating five pentamers. Open, large circles denote the hydrophilic head monomer in the pentamers, filled circles denote hydrophobic tail monomers, the small circles denote water molecules (note that all the molecules have the same ''size'' in the simulation; they differ only in this graphical representation).

tional information for orienting or aligning the polymers in a well-defined way, as shown in the next subsection.

2. Lipidlike pentamers in a polar environment

The present LMA setup is already very sensitive to the variation of the molecular types involved in the dynamics. Figure 8 shows intermediates of simulating lipidlike polymers [as schematically shown in Fig. 1(c)] in the polar environment. The hydrophilic head monomers in the pentamer are indicated by the open, large circles, the hydrophobic tail monomers by the filled circles. The small circles indicate water molecules. The topology of these clusters [(a) 10^3, (b) 5.10^4, and (c) 10^5 updates], as well as their formation dynamics, especially with respect to a long time scale needed to form clusters (as discussed in Sec. IV E), differs strongly from the example shown in Fig. 7. These clusters [the dimeric associates in Figs. 8(a) and 8(b) as well as the quatermeric in Fig. 8(c)] are ordered in such a way that the hydrophilic head monomers always stay in contact with water, whereas the hydrophobic tails try to cluster. This example shows that even a slight variation of the physicochemical type of only one monomer in the pentamer essentially changes the cluster formation process.

Thus there is a crucial dependence of the macromolecular aggregation on the chemical type of the molecular entities involved. To ensure proper functionality of higher-order structures composed by supramolecular ensembles, specific information has to be present on the basic molecular entities. The higher the order is and the more specific a task of a biological structure is, the more information has to be present at the underlying chemical entities to specify the structure and thus its functionality [4].

3. Polymer update on a two-dimensional lattice

The treatment of polymers in the present LMA setup is confronted with two basic problems: on the one hand, the dimensionality of the lattice and on the other hand, the parallel update of an extended object based only on local, discrete rules.

(a) Dimensionality. A two-dimensional lattice is sufficient to simulate monomeric fluid flow in a qualitative and quantitative correct way, as also demonstrated by the results of the lattice gas automata simulations formulated in two dimensions [24]. Due to the bonds and the excluded molecular volumes, polymers reduce the degrees of freedom in their vicinity for other monomers significantly. A straightforward simulation of polymers and solvent in the LMA yields typical dimension-based phenomena in the solvent structure

around polymers, e.g., dense clustering. To avoid these effects and to study solvent properties in ''local three dimensions,'' a second lattice can be introduced to allow solvent molecules to pass positions occupied by monomers in polymers if they are not bonded to any other molecule (or, more exactly, if their thermal state is higher than their yield of binding energy on the present position). This second lattice corresponds to a solvent reservoir. If a solvent molecule enters the second lattice, an identical solvent molecule, with respect to relative orientation and thermal state, is released onto a free work-lattice position in the move direction of the particular solvent molecule. We used this approximation in the above-discussed simulation of polymers.

(b) Parallel polymer update. The real-time movement of a polymer is an intrinsically parallel process. In a physical system the translational state of a subpart (monomer) of the polymer in time t is instantaneously (with the speed of light) known to all other subparts. To realize this global information flow, at least $l-1$ propagation steps in a polymer of the length l have to be performed in the LMA. To resolve possible conflicts requires additional information propagation steps. For a more detailed discussion of these issues we refer to [22,1]. A polymer in the LMA is characterized by an elastic deformability of the monomers in a collision process. The information about the energetic state of a monomer is only propagated to the bond neighbors (i.e., monomers in NH1) in the chain in one time step, assuming that the propagation of the momentum along the chain is slow (one site per time step) due to the time lack based on the deformation of subunits (librational and vibrational modes of bonds). The same feature also holds for the LMA solvent molecules, where momenta are also only propagated to neighborhood 1 in one time step. This is because a simultaneous fulfillment of (i) a strict parallel update, (ii) strict local interaction rules, and (iii) a strict conservation of momentum, is not possible [27]. For other cellular-automata-based polymer updating methods we refer to [28,29].

E. Correlation of LMA updates to a physical time scale

The representation of a LMA simulation in an absolute time scale can only be roughly estimated. The overall relaxation times of polar liquids, determined, e.g., by ultrafast

fluorescence spectroscopy [30], are in the range of one pico-second. The underlying processes in this time regime are the dynamics of fast, mainly librational and rotational, modes in between 10 and 100 fs, followed by a slower, longitudinal relaxation up in the picosecond range.

The longitudinal relaxation in our lattice model is defined by the translation of a particular water molecule from one lattice site to a site in neighborhood 1. On average three full updates of the lattice are needed to translate one water molecule (at the given global proportionality factor of 3.7). These three updates could now be assigned to a 1-ps time step. Following this interpretation, the first two updates correspond to librational and rotational modes of the LMA water molecule (i.e., rotation of a molecule on a given lattice site) and the third update is on average the translational contribution to the relaxation time.

The update of a hydrophobic monomer in bulk water is comparably faster, on average two updates, which correspond to one translational relaxation. The relaxation time of a hydrophilic monomer is near the relaxation time of water in our model. The exact values for the system with $a_{global}=3.7$ are 3.3 updates for water, 3.0 updates for hydrophilic monomers, and 1.9 updates for hydrophobic monomers in the bulk water phase. However, all calculated monomer systems show a comparable update time in the range of fewer than 4 updates and, related to a time scale, a longitudinal relaxation time should be in the range of 1 ps.

The time for updating the model pentamers is, due to the constraints introduced by bonds, much longer. A full translational polymer update, and the corresponding translational relaxation, is defined by at least one translation of each monomer in the polymer by a distance one on the lattice. The translational relaxation of a hydrophilic pentamer takes on average 1.5×10^4 LMA steps, of a hydrophobic pentamer 6×10^3 (see Fig. 7), and of a lipidlike pentamer, as show in Fig. 8, 1.2×10^4 LMA update steps. These numbers of update steps correspond, taking the update of a single water molecule as reference (where three updates correspond to 1 ps), to 4–5 ns for the hydrophilic, 2 ns for the hydrophobic, and 4 ns for the lipidlike pentamer, respectively.

Surprisingly, the translational relaxation of a lipidlike pentamer is similar to the time range of a hydrophilic pentamer, although only one monomer in the pentamer is hydrophilic. This decreased flexibility of lipidlike polymers, compared to hydrophobic polymers, is also reflected by an increased cluster stability (Fig. 8) compared to hydrophobic clusters (Fig. 7).

In general, the translational update times or polymers in the LMA model seem to be overestimated. This is probably mainly due to the reduced number of degrees of freedom when simulating polymer dynamics on a two-dimensional grid. The simple molecular dynamics and molecular self-assembly simulation discussed here are thus typically simulated up to the order of 0.1 μs real time and they are easily performed on a personal computer or a small workstation.

V. THERMODYNAMIC CHARACTERIZATION OF THE LMA

The driving force for dynamics within the LMA is formally based on two (in the simulation, strictly separated) basins of energy: (i) the thermal state of a molecule, consisting of translational energy and energy distributed over inner degrees of freedom within a molecule, e.g., rotational terms, is either stored on inner degrees of freedom during the free translation or distributed to other molecules in a collision process and (ii) the potential energy between specific sites on the three molecular entities recruiting attracting and repelling forces. Binding of a molecule influences the occupation time of a molecule on a particular lattice location. If the highest kinetic energy in a direction exceeds the sum binding energy of the molecule the intermolecular bond breaks. However, the sum inner energy on the molecule remains unchanged.

Monomers in the LMA can be interpreted as an ideal gas if all occupied data structures (or lattice sites) are separated by at least a neighborhood of 3. In this case, the total energy of the system E_{total} is given by the sum kinetic energy K_{total}. Compressing this ''ideal gas'' to the (constant) simulation volume results in a decrease of the potential energy $-V_{b,total}$ as intermolecular interactions are realized and bonds are formed. The decrease of this potential energy during the simulation, based on the ''optimization'' of the intermolecular interactions and depending on the global proportionality factor a_{global}, is *implicitly stored as inner (intermolecular) energy*. Note that the distribution of the kinetic energies in each direction as well as K_{total} itself is not changed in time. Thus all occurring energy losses are not considered explicitly, but the inner energy provides the necessary energy whenever a bond is broken. Recall that the decrease of this potential energy during the simulation, due to the bond formation and depending on the global proportionality factor a_{global}, is implicitly stored as inner intermolecular energy and that it can always be recovered again as molecular assemblies are broken up.

The total energy of the system is thus given by

$$E_{total} = K_{total} + V_0 = \text{const}, \qquad (9)$$

where V_0 is the potential energy or binding energy term when the simulation is started. The system has a constant total energy. The total number of grid points on the lattice, i.e., the volume, and the total number of molecules are also constant during the simulation. Thus the LMA confirms to a *microcanonical ensemble*.

The above interpretation allows the formal definition of the entropy as

$$S = k_{system} \ln Z, \qquad (10)$$

where k_{system} is a LMA intrinsic constant corresponding to the Boltzmann constant k_B for a physical system and Z is a partition function over the states of the molecules in the simulation. Since Z is not known explicitly (we would have to derive the Hamiltonian for the LMA) an approximation of the entropy S_{LMA} can easily be calculated. S_{LMA} measures an occupation pointer as an approximation to the partition function of n molecules on the lattice and does not explicitly take the particular energetical states of a molecule into consideration:
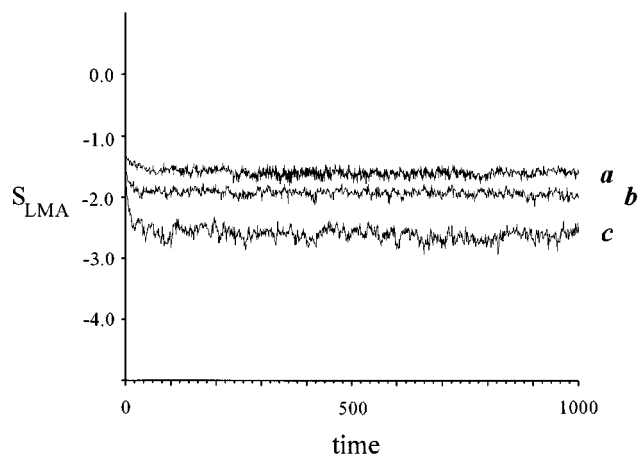
FIG. 9. Evolution of entropy, as formulated in Eq. (11) (see the text), for the first 1000 updates of a water simulation, curve a, and two mixtures of water and hydrophobic monomers: curve b, 16% hydrophobic monomers, 34% water, 50% empty; and curve c, 25% hydrophobic monomers, 25% water, 50% empty.

$$S_{\mathrm{LMA}}(t) = k_{\mathrm{system}} \ln \frac{\sum_{i=1}^{n} D_i}{n}, \qquad (11)$$

where D_i is an occupation pointer of molecule i with the value 0, if the molecule does not change its location (i,j) on the lattice between time t and $t+1$, and 1 if the molecule changes the position in one update.

This definition of entropy only considers the location parameter of the generalized coordinates Γ, but not explicitly the entropic impact of the distribution of energetic states, as noted for a general partition function in Eq. (10). But, as we will see below, this *positional* or *structural* entropy is the manifestation of the specific energetic state of monomers in given neighborhood situations.

In the case of the ideal gas LMA in an infinite simulation volume (no interaction between molecules, no excluded volumes), the sum over all D_i is equal to n and the entropy is therefore zero for this reference system. Figure 9 shows the dynamics of entropy as defined in Eq. (11) for water and water:hydrophobic monomer mixtures. The corresponding energetic implication for the systems shown in Fig. 6(b) (25% water, 25% hydrophobic monomer mixture) compared to a water simulation (shown in Fig. 4) is given in Fig. 10. The decrease of entropy (S_{LMA}), based on the stabilization of molecules by bond formation, is especially monitored during the first 100 steps of the simulation of a water system (curve a) and the two water:hydrophobic monomer mixtures (curves b and c), as shown in Figs. 6(a) (16% hydrophobic monomers) and 6(b) (25% hydrophobic monomers). The mean entropy for the water system is -1.55 and remains constant also after longer simulation times. The entropy is lower for the mixtures: -1.9 for system b (16% hydrophobic monomers) and -2.5 for system c (25% hydrophobic monomers). These values continue to decrease, e.g., the respective values for system b are -1.95 after 10^3 simulation steps and -2.65 after 10^5 steps. This again reflects the comparably slow phase-separation process for the mixtures.
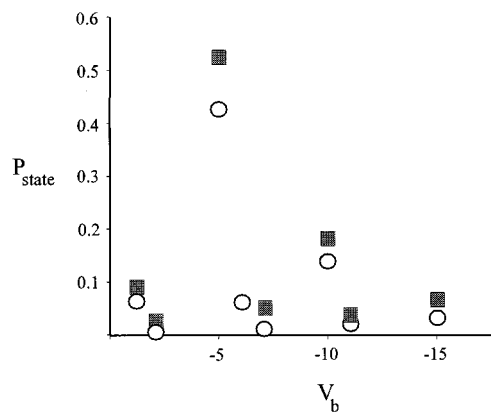
FIG. 10. Probability P_{state} of finding a particular water molecule with a certain binding energy in the range $[0,-18]$. P_{state} values below 0.02 are not shown. Open circles denote P_{state} values for molecules in bulk water (as in the system shown in Fig. 4), filled squares denote P_{state} values for water molecules in a mixture neighboring at least one hydrophobic monomer [equal concentration; see also Fig. 6(b)].

The entropy, as defined in Eq. (11), is generally lower for the mixtures compared to pure water and depends on the concentration of hydrophobic monomers in the system, since the value of S_{LMA} is lower for c compared to b. This is especially of interest when considering the a_{global} values, 3.7, 4.4, and 4.2, for the three systems (as discussed in Secs. IV B and IV C). These values indicate the opposite behavior—a general *destabilization* of molecules in a mixture and a concomitant *increase of entropy*—since an increase in $K_{\mathrm{total}}/V_{b,\mathrm{total}} = a_{\mathrm{global}}$ is observed.

This increase is mainly based on the fact that the loss of H bonds between water molecules is not completely counteracted by dipole–induced-dipole and induced-dipole–induced-dipole interactions (see Sec. IV C). The reason for clustering and the decrease of entropy is based on the *local* (and not the global, as indicated by a_{global}) distribution of energetic states, which is not explicitly considered in Eq. (11) or Fig. 9.

Figure 10 denotes the probability P_{state} to find a water molecule with a particular binding energy ranging from -1 to -18 (three H bonds, three dipole–induced-dipole interactions). The open circles denote the P_{state} values for water molecules in bulk water phase (as in Fig. 4). Three main peaks are found at -5, -10, and -15, corresponding to the three possible hydrogen bonds on one particular water molecule. The same overall distribution is also found for the mixture with 25% hydrophobic and 25% water molecules on the lattice [see also Fig. 6(b)]. The P_{state} values calculated for water molecules neighboring at least one hydrophobic monomer are denoted by the filled squares in Fig. 10.

The difference in the mixture is the change in the overall probability of water to form a hydrogen bond: Especially water molecules in the neighborhood of hydrophobic monomers are on average stabilized to a higher extend, mainly at the binding potential of -5 ($P_{\mathrm{state}}=0.53$ for water neighboring hydrophobic molecules, 0.42 for water neighboring water).

This inhomogeneous, local distribution of binding energies is the reason for the decrease of entropy for the mixture systems. It is the reason for the entropy decrease shown in curves b and c in Fig. 9. This finding indicates the formation of comparably stable structures around hydrophobic clusters and therefore a slower dynamics in the vicinity of hydrophobic surfaces. This finding corresponds to the experimentally determined decrease of entropy when solvating hydrophobic molecules at room temperature and is in accordance with other models describing hydrophobic effects showing slow dynamics of water molecules in the hydration shell of hydrophobic surfaces [31–33].

It should be noted that the phase-separation process of hydrophobic monomers in a polar environment and the concomitant decrease of entropy are not explicitly implemented properties of the molecular elements in this simulation. They are the *result* of the system dynamics. These hydrophobic effects are thus *emergent properties* of the molecular dynamics.

VI. CONCLUSION

We have presented a different type of molecular dynamics and self-assembly simulation, the lattice molecular automaton, that is able to handle very large molecular systems over long times (up to the range of seconds). In the LMA all interactions (electrostatic forces) are decomposed and communicated via propagating force particles or ''photons.'' The monomer-monomer bond forces, the molecular excluded-volume forces, the longer-range intermolecular forces, the polymer-solvent interactions, and the solvent-solvent interactions are all modeled by propagating information particles.

The concept of lattice data structures, sharing locally propagated information, is the basis for this kind of molecular dynamics and self-assembly simulation. The data structures are interpreted as computational nodes, storing type-specific characteristics of molecules as water, hydrophilic, and hydrophobic monomers. The update of the state of the data structures at each lattice site is based on the local information and the received (propagated) information from a given neighborhood on the discrete lattice.

The LMA is a tool that enables the study of the principle physical mechanisms that generate higher-order molecular structures.

(i) A polar solvent like water is characterized by clustering of water molecules in a hydrogen bonded network with fast rearrangement dynamics. The water structures generated in the LMA produce the same radial distribution function as experimentally measured.

(ii) The hydrophobic effect, which is not explicitly encoded in the LMA, is correctly *generated* by the interactions between the hydrophobic monomers and the water molecules.

(iii) Phase separation of hydrophobic monomers in water in the LMA system follows the same dynamical characteristics as have been experimentally determined. This clustering dynamics is, based on the high binding energies of hydrogen bonds, feasible from the enthalpic point of view, but not for the entropic state of the system. The structural features of liquid water are in a sensitive balance of entropy and enthalpy. The dissolution of hydrophobic particles exactly in-fluences this balance. The consequence of this perturbation, the *generated* hydrophobic effect, drives the phase separation of hydrophobic molecules in a polar environment.

(iv) LMA lipid polymers form ordered, higher-order molecular structures in water.

(v) The discrete, microscopic system representation, which enables a direct calculation of thermodynamic properties of a microcanonical ensemble, gives a direct way to compare results from simulation with thermodynamic data from experiments and further determine how different microscopic effects contribute to the macroscopic thermodynamic quantities. The change of entropy during solvation processes can, for instance, directly be followed in the LMA system.

(vi) The molecular water structures around hydrophobic surfaces can be directly inspected and the entropic changes followed.

Vesicles and micellelike structures are typical examples of higher-order molecular structures that can be generated by lipid:water mixtures. The driving force for the phase separation and ordering of lipids in water is the hydrophobic effect, which is a result of the interactions of the hydrophobic and hydrophilic molecules arranged in polymers and the polar water molecules. Minimal physicochemical properties of molecular entities represented as information in data structures on the two-dimensional lattice allows the LMA system to have constructive dynamics and generate higher-order molecular structures, e.g., ordered lipid aggregates.

The data structure concept of the LMA is of course expandable to represent more details of the Physics so that yet higher-order interactions and thus structures can be generated. (We use the term Physics to denote the real world and not our models of the real world, which we denote physics.) It should, for instance, be possible to have ''membrane proteins'' to assemble into the vesicles so that a transport of molecules becomes possible, perhaps to fuel a chemical reaction inside the vesicle that can change the vesicle [8]. Also an assembly of larger molecular units, e.g., whole micellular entities, is possible by appropriate expansion of the data structure.

As we may in this way step up into the dynamical hierarchy of molecular structures, the computational resource requirements will eventually explode and we will be forced to change the level of description if we want to understand the dynamics of these processes. We would need to go to a higher level of description and now interpret each data structure as a molecular aggregate itself and change the data structure appropriately. Science has to a large extent been successful by doing exactly that: choosing appropriate levels of description. With the LMA we have developed a simulation tool that allows us to investigate the dynamics of the generation of molecular hierarchies, which are processes that are not well understood.

[1] B. Mayer and S. Rasmussen, Technical Report, LA-UR 96-1732 (unpublished).

[2] R. B. Gennis, *Biomembranes* (Springer, Berlin, 1988).

[3] N. A. Baas, in *Artificial Life III*, Proceedings of SFI Studies in the Science of Complexity, edited by Ch. G. Langton (Addison-Wesley, Reading, MA, 1993), Vol. XVII, p. 515.

[4] N. A. Baas, M. W. Olesen, and S. Rasmussen, Technical Report, LA-UR 96-2921 (unpublished).

[5] Sh. Chiruvolu, S. Walker, J. Israelachvili, F. J. Schmitt, D. Leckband, and J. A. Zasdzinski, Science **264**, 1753 (1994).

[6] H. Hotani, R. Laholz-Beltra, B. Combs, S. Hammerhoff, and S. Rasmussen, Nanobiology **1**, 67 (1992).

[7] J. Tabony, Science **264**, 245 (1994).

[8] T. Oberholzer, R. Wick, P. L. Luisi, and Ch. Biebricher, Biochem. Biophys. Res. Commun. **207**, 1 (1995); **207**, 250 (1995).

[9] J. A. Tuszynski, H. Bolterauer, and M. V. Sataric, Nanobiology **1**, 177 (1992).

[10] Ch. Tanford, Science **200**, 1012 (1978).

[11] L. R. Pratt, Annu. Rev. Phys. Chem. **36**, 433 (1985).

[12] P. Rossky, Annu. Rev. Phys. Chem. **36**, 321 (1985).

[13] A. Henn and W. Kautzmann, J. Phys. Chem. **93**, 3770 (1989).

[14] J. T. Pedersen and J. Moult, Curr. Opin. Str. Biol. **6**, 2 (1996); **6**, 227 (1996).

[15] W. F. van Gunsteren, J. F. Luque, and P. Timms, Annu. Rev. Biophys. Biomol. Struct. **23**, 847 (1994).

[16] S. Kirkpatrik, C. D. Gelatt, and M. P. Vecchi, Science **220**, 671 (1983).

[17] R. L. Jernigan and I. Bahar, Curr. Opin. Str. Biol. **6**, 2 (1996); **6**, 195 (1996); P. Koehl and M. Delarue, *ibid*. **6**, 2 (1996); **6**, 222 (1996).

[18] P. Privalov and S. J. Gill, Adv. Prot. Chem. **39**, 191 (1988).

[19] Ch. T. Klein, B. Mayer, G. Köhler, and P. Wolschann, THEOCHEM, J. Mol. Struct. **370**, 33 (1996).

[20] T. Solmajer and E. L. Mehler, Int. J. Quantum Chem. **44**, 291 (1992).

[21] G. Böhm, Chaos, Solitons Fractals **1**, 4 (1991); **1**, 375 (1991).

[22] S. Rasmussen and J. R. Smith, Ber. Bunsenges. Phys. Chem. **98**, 9 (1994); **98**, 1185 (1994).

[23] K. A. Dawson, in *Structure and Dynamics of Strongly Interacting Colloids and Supramolecular Aggregates in Solution*, edited by S.-H. Chen, J. S. Huang, and P. Tartaglia (Kluwer, Dordrecht, 1992), p. 265, and references cited therein.

[24] U. Frisch, B. Hasslacher, and Y. Pomeau, Phys. Rev. Lett. **56**, 1722 (1986).

[25] S. K. Burley and G. A. Petschko, Adv. Prot. Chem. **39**, 125 (1988).

[26] B. Hasslacher, *Discrete Fluids* (Los Alamos National Laboratory, Los Alamos, 1987).

[27] Y. Bar-Yam (private communication).

[28] B. Chopard, J. Phys. A **22**, 1671 (1990).

[29] O. Ostrovsky, M. A. Smith, and Y. Bar-Yam, Annu. Rev. Biophys. Biomol. Struct. **24**, 239 (1995).

[30] M. Marconelli, J. Mol. Liq. **57**, 1 (1993).

[31] D. A. Zichi and P. J. Rossky, J. Chem. Phys. **84**, 2814 (1986).

[32] P. J. Rossky and M. Karplus, J. Am. Chem. Soc. **101**, 1913 (1979).

[33] H. Tanaka and K. Nakanishi, J. Chem. Phys. **95**, 3719 (1991).